Heliyon 7 (2021) e07211

Contents lists available at ScienceDirect

Heliyon

journal homepage: www.cell.com/heliyon

Research article

COVID-19 pulmonary consolidations detection in chest X-ray using progressive resizing and transfer learning techniques

Anant Bhatt [a], Amit Ganatra [b], Ketan Kotecha [c,*]

[a] Centre of Excellence- AI, Military College of Telecommunication Engineering, Mhow, India
[b] Devang Patel Institute of Advance Technology and Research, Charotar University of Science and Technology, Changa, India
[c] Symbiosis Centre for Applied Artificial Intelligence, Symbiosis International (Deemed University), Pune, India

ARTICLE INFO

Keywords:
COVID-19
Chest X-ray analysis
Pulmonary consolidations
Transfer learning
Progressive resizing
Saliency maps

ABSTRACT

A viral outbreak with a lower respiratory tract febrile illness causes pulmonary syndrome named COVID-19. Pulmonary consolidations developed in the lungs of the patients are imperative factors during prognosis and diagnosis. Existing Deep Learning techniques demonstrate promising results in analyzing X-ray images when employed with Transfer Learning. However, Transfer Learning has its inherent limitations, which can be prevaricated by employing the Progressive Resizing technique. The Progressive Resizing technique reuses old computations while learning new ones in Convolution Neural Networks (CNN), enabling it to incorporate prior knowledge of the feature hierarchy. The proposed classification model can classify pulmonary consolidation into normal, pneumonia, and SARS-CoV-2 classes by analyzing X-rays images. The method exhibits substantial enhancement in classification results when the Transfer Learning technique is applied in consultation with the Progressive Resizing technique on EfficientNet CNN. The customized VGG-19 model attained benchmark scores in all evaluation criteria over the baseline VGG-19 model. GradCam based feature interpretation, coupled with X-ray visual analysis, facilitates improved assimilation of the scores. The model highlights its strength to assist medical experts in the COVID-19 identification during the prognosis and subsequently for diagnosis. Clinical implications exist in peripheral and remotely located health centers with the paucity of trained human resources to interpret radiological investigations' findings.

1. Introduction

World Health Organization (WHO) reported viral emergences over numerous occurrences, which epitomizes a severe concern for public health. In the last two decades, viral epidemics like Severe Acute Respiratory Syndrome Coronavirus (SARS-CoV), H1N1 influenza, and the Middle East Respiratory Syndrome CoronaVirus (MERS-CoV) have drawn significant attention. In November 2019, a similar viral outbreak with a lower respiratory tract febrile illness was reported in China. Bronchoalveolar lavage (BAL) test analysis highlighted an unfamiliar coronavirus strain responsible for the outbreak. The World Health Organization named the pulmonary syndrome "COronaVIrus Disease 2019" (COVID-19) or severe acute respiratory syndrome coronavirus2 (SARS-CoV-2). The cumulative number of confirmed cases crossed 14,79,168 globally, with approximately 87,987 virus-related deaths as of April 09, 2020, with a significant spread worldwide [1].

Etiological tests, Reverse-Transcription Polymerase chain reaction test, Chest X-rays, and Chest Computed Tomography Scans (CT-Scans) are the tests/techniques which can identify the infection. A nasopharyngeal Exudate swab sample is screened in the RT-PCR test. However, the RTPCR test's reliability with higher turnaround time poses a challenge in diagnosis, especially in developing nations due to limited medical facilities. As the infections in the lungs can be screened with radiographs, the radiographs are being used in the diagnostic workup, check disease progression, and follow-up of the pulmonary consolidations. Since the coronavirus consolidation is dissimilar to bacterial or viral pneumonia consolidation, the radiographs help identify the COVID-19 infection. The chest X-ray findings can improve the diagnosis time-cycle with enhanced screening capability. It also helps to prioritize the treatments of the patients at hospitals. Hence, X-ray analysis is a discriminative element that assists in the timely identification of COVID-19 infections.

* Corresponding author.
E-mail addresses: capt.anant@gmail.com (A. Bhatt), drketankotecha@gmail.com (K. Kotecha).

https://doi.org/10.1016/j.heliyon.2021.e07211
Received 2 June 2020; Received in revised form 13 September 2020; Accepted 1 June 2021

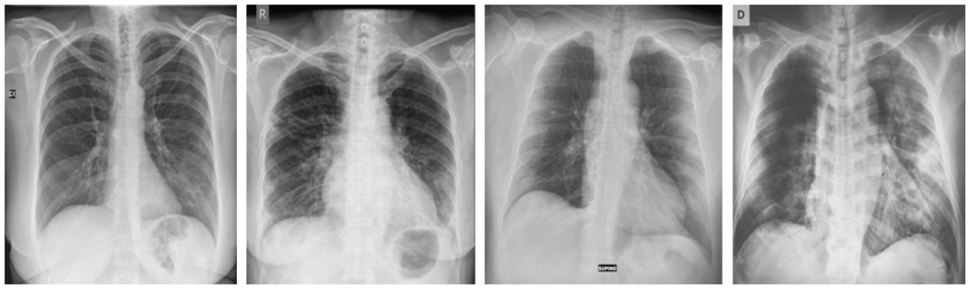

Fig. 1. The figure shows Chest X-rays from the dataset indicating typical subpleural peripheral Opacities [9].

Table 1. The table illustrates essential aspects of the existing literature for detection of COVID-19 consolidation are shown in the table, which uses various approaches. (Abbreviations: CNN- Convolution Neural Network, SVM- Support Vector Machine, VGG- Visual Geometry Group, and Acc- Accuracy.)

Literature	COVID	Pneumonia	Normal others	Class	CNN/Algo	Acc %
[10]	127	500	500	3	DarkNet	87.02
[11]	142	–	142	2	nCOVnet	88.10
[12]	25	–	25	2	InceptionV3, VGG19, Xception, MobileNetV2, DenseNet201, InceptionResNetV2, ResNetV2,	90.00
[13]	105	11	80	3	DeTraC	95.12
[14]	168	-	168	2	Custom CNN	96.13
[15]	162	–	1583	2	ResNet50, InceptionV3, Truncated Inception	94.04
[16]	130	99	31	3	Shallow ConvNet	96.92
[17]	295	98	65	3	MobileNetV2, SqueezeNet, SVM	99.27

Since the etiologic and clinical physiognomies of the illness are analogous to those of SARS and MERS, the experience of these pulmonary syndromes can be helpful during the diagnosis of the COVID-19 [2, 3, 4, 5, 6]. The X-ray images with an exposure of SARS, MERS, pneumonia, and COVID-19 have been taken to develop the X-ray analysis model using Convolution Neural Networks to identify COVID-19 chest infections. The findings are referred to as Ground Glass Patterned areas, which indicate COVID-19 infection. The infections affect both lungs, particularly the lower lobes, especially the posterior segments, with a fundamentally peripheral and subpleural distribution. With visuals of Lesions progression, septal thickening, and formation of Crazy Paving Pattern or Ground Glass Pattern (rounded morphology), the X-ray can indicate the infection [7, 8]. Fig. 1 shows the visual distinction in the same patient's chest X-rays with typical subpleural peripheral opacities developed due to COVID-19 infections.

Our work is motivated by Convolution Neural Network models' convincing performance and the prevailing need for an alternate screening methodology for an efficient healthcare ecosystem for timely detection of COVID-19. We carried out studies on the work published by various research groups. We have carried out a comparative analysis, which brings out the dataset insights, a number of classes, type of Deep Learning models, and performance of these experiments, and details are covered in Table 1. Most of the work has been done on small-sized datasets due to the inadequate availability of annotated Chest X-Rays. However, some of these research groups have used augmented/selective Chest X-Ray images. We also studied data augmentation techniques used in different variants of the investigation.

The majority of the published work incorporates two or three-class classification with binary classification. We have analyzed various CNN models by studying their performance scores and the methodology. Since the Convolution Neural Networks (CNN) do not have predefined kernels and learn locally from connected neurons representing data-specific kernels, the CNN filters can be applied repeatedly to the images to classify the X-ray images. We conclude from the study that suitable CNNs can be employed to carry out multi-class classification with an unskewed balanced dataset. We propose the Transfer learning technique's employment on the X-Ray databases. The technique enhances learning new tasks and enables improved classification by transferring learned knowledge from relevant classification datasets. We first train a baseline COnvolution Neural Network on a base dataset with the defined task. After obtaining the weights, we repurpose the learned features by transferring this knowledge to a target (X-ray analysis) model, which will be trained on the X-ray dataset. Transfer Learning helped reduce training time and improve neural network performance. However, this technique also suffers from inherent limitations of negative transfer and overfitting. We propose a novel implementation methodology by amalgamating the Progressive Learning technique with the Transfer Learning technique to circumvent the limitations. The Progressive Resizing technique reuses old computations while learning new ones in Convolution Neural Networks (CNN), which enables it to incorporate prior knowledge of the feature hierarchy [18]. The paper proposes a novel methodology to detect the COVID-19 pulmonary consolidations in X-ray images with a method to interpret the CNN analysis with intuitive Saliency maps (GradCam) Visualisation. Our contributions are listed as follows:

- We present a novel Classification Model to detect COVID-19 pulmonary consolidations in chest X-ray, achieving the best specificity and sensitivity score.
- We propose a modified VGG-19 architecture that shows promising results over the Baseline VGG-19 model when applied with the Transfer Learning technique.
- We demonstrate a comparative analysis of the results generated by CNN models with various techniques.

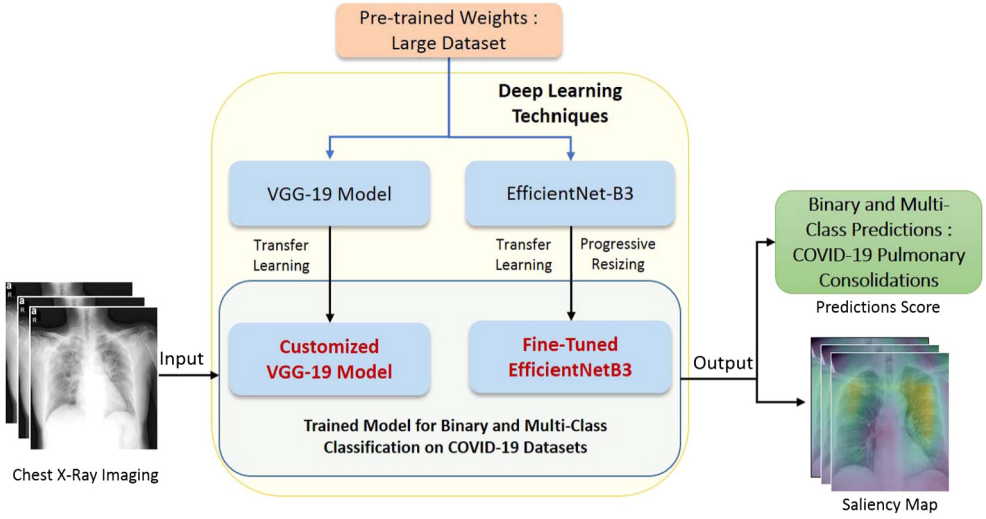

Fig. 2. The figure illustrates the implementation methodology and the inference pipeline with the employment of Transfer Learning and Progressive Resizing Techniques on ConvNets to detect COVID-19, Pneumonia consolidations in the X-rays with the saliency maps.

- The classification models classify the X-ray in Pneumonia, SARS-CoV-2, and Normal X-ray with GradCAM Saliency Maps for enhanced assimilation.

2. Datasets

The classification scores are impacted by volumetric data of one class and may skew away from the severity of coronavirus influence while analyzing the radiology images. Hence, the use of multitudinal and multimodal is done while designing a robust AI model [14]. There is a bright possibility of increasing diagnostic results using different clinical data of the same patients, i.e., Electronic Health Record (EHRs), computerized tomography (CT) scans, and Chest X-rays. However, the availability of such a dataset for making an AI model is a challenge. Hence, we have carefully studied the chest X-Rays to formulate our experiments. We used the X-ray Imaging dataset of the COVID-19 patients for the experiments, which was curated by Dr. Joseph Cohen of the University of Montreal, Canada [9]. The dataset incorporates Normal, and COVID-19 infected X-Ray images. We used the COVIDx Dataset of the COVID-Net Team (Vision and Image Processing Research Group), University of Waterloo, and Darwin AI Corp, Canada [19]. The X-Ray imaging dataset consists of 16,756 chest radiography images, including 66 X-ray images of COVID-19. High skewing observed in the quantity of X-ray appertaining to Normal, Pneumonia, and COVID-19 classes may impact the classification scores while training CNNs. Hence, we created a balanced, relevant dataset in consultation with a radiologist to carry out experiments for multi-class classification. The composite dataset has 100 X-rays each in healthy and pneumonia classes and 104 X-ray images of the COVID-19 class.

3. Implementation and methodology

We conducted our experiments on Dr. Joseph Cohen's and amalgamated datasets for binary and multi-class classifications. We conducted the experiments on Convolution Neural Network models, i.e., VGG-19 (baseline) and customized VGG-19 [20], and EfficientNet-B3 Neural Network [21]. To improve the baseline models' results, we incorporated modifications in the final layers of these CNNs. We employed the Transfer Learning technique by transferring pre-trained weights from the ImageNet dataset [22, 23] and then superimposed the Progressive Resizing technique while training the designated CNN models on X-ray imaging datasets. Finally, the classification experiments demonstrated improvements in the results for both datasets. GradCam based Saliency maps facilitate X-ray imaging analysis by highlighting relevant visual information with classification scores. Fig. 2 illustrates the proposed Methodology to detect COVID-19 and Pneumonia in X-ray imaging and generate Saliency Map. We conducted our experiments on Nvidia GTX 2080Ti GPU (4352 CUDA cores). Our experiments and implementation methodology incorporates four stages, i.e., Data Preprocessing, Model Implementation, Training Strategy, and Testing.

3.1. Data preprocessing

We have employed data augmentation techniques to generate X-ray variations from the available X-ray imaging due to the limited availability of annotated X-ray images of COVID-19 infected patients. The variations were incorporated into the dataset during the training and validation phases. During data processing phase, we used the value of θ = -60 to 60 degrees, α = 1.0 - 1.1, P_A = 0.75 and P_B = 0.5. We used the following techniques to process the data and augment the datasets:

- Horizontal Flipping of the X-rays imaging with a probability of P_B.
- X-Ray rotations were carried out due to rotational invariance.
- Random scaling of α was applied with a probability of P_A.

3.2. Model customization and implementation

COVID-19 Chest X-ray exposes palpable white patches in the lungs – referred to as Ground-Glass-Windows. The proposed CNN approach deliberates on varied patterns like Consolidation, Interstitial, Nodules/masses, and Atelectasis observed in the X-rays. Transfer learning and domain adaptation help to use the knowledge learned in one setting to improve generalization in another setting. During the employment of Transfer Learning, we used pre-trained weights obtained after training the model on a large dataset (i.e., ImageNet) while re-training the model on the COVID-19 datasets. We carefully optimized relevant Hyperparameters, which govern the training process and affect network structure. Learning Rate was optimized after each epoch using an LR finder that identified the optimal learning rate for the subsequent epochs. Various experimental results determined the number of Epochs. We explored various activation functions during the experiments, i.e., ReLU, SoftMax, and TanH. The values of the hyperparameters were optimized during experiments. The Progressive Resizing technique was used repeatedly with a progressive increase of the size of the x-ray images. The methodology facilitated the effective extraction of the features in each iteration, thereby attaining the optimum weights. The same methodology was applied while carrying out multi-class classification

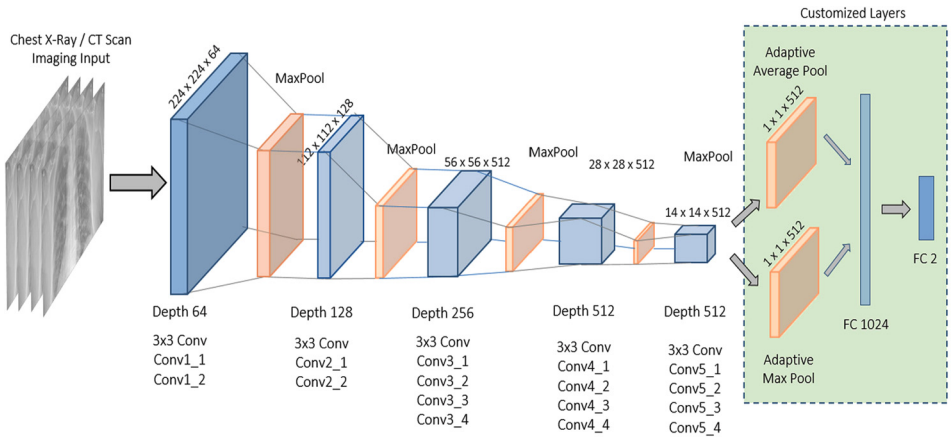

Fig. 3. The figure illustrates Customized VGG-19 Architecture tailored to detect COVID-19, Pneumonia Consolidation in Chest X-Ray Imaging. The modified 'Head' block in the architecture conserves stability between computational efficiency and representational capacity during binary and multi-class classification.

on the amalgamated dataset, containing images with pneumonia consolidation.

3.2.1. Customized VGG-19

We used the Baseline VGG-19 model for our experiments on both datasets. We have carried out binary and multi-class classification. We carried out modifications to the baseline VGG-19 model to attain improved results. In VGG-19 baseline model, 'Backbone'- convolution layers analyse the X-ray consolidation features. These layers are dovetailed by culminating linear layers, referred to as 'Head.' 'Head' translates the analyzed features during generating prediction scores for two classes in binary classification. To reduce the learning time and optimize the learning of the CNNs, we employed differential learning rates. We split the head from the rest of the architecture layers and ran the experiments on 'Backbone.' To carry out relevant modifications in VGG-19 architecture, we replaced the 'Head' with the AdaptiveConcatPool layer with Flatten Layer, blocks of Batch Normalization, Dropout, Linear, and ReLU layers. We appended two units with softmax activation as a fully connected layer referenced as - 'Final Classification Layer.' This AdaptiveConcatPool Layer effectively preserves the backbone's feature representations compared to using only the MaxPool Layer or the AveragePool Layer in the 'Head.' Fig. 3 shows a novel modified VGG-19 architecture which demonstrated a substantial upsurge in outcomes.

3.2.2. EfficientNet B3

EfficientNet is a CNN architecture and has several variants. It is a scaling method that uniformly scales all dimensions using a compound coefficient. Since the more extensive networks with greater width, depth, or resolution tend to achieve higher accuracy, we used EfficientNet for carrying out multi-class classification. These models demonstrated enhanced performance during the experiments. Output layers of these CNN variants were suitably modified for classification experiments on both datasets.

3.3. Training strategy

We used pre-trained weights while employing Transfer Learning to train the VGG-19 and Customised VGG-19 CNN models. We experimented with the proposed novel methodology using the Transfer Learning technique followed by the Progressive Resizing while training EfficientNetB3 models. We carried out experiments on the datasets with training to test subsets as 80:20. We used the Discriminative Learning strategy to extract relevant features' information while training the models. We used Weight decay (Wd) to guard against overfitting, which prevents the weights from growing too large. We used Binary Cross Entropy as the loss function. We changed the learning rates iteratively by using the LR Finder [24] on each set of experiments. We used a 1-cycle policy to optimize the learning rates, which helped achieve Super-Convergence with faster training, ensuring optimum regularization [25, 26].

3.3.1. VGG-19 models

The baseline model of Very Deep Convolutional Networks is used in our multi-class classification. It attains a significant accuracy on image classification and localization tasks. Due to its inherent strength in processing X-Ray image recognition, we used it for our experiments. We implemented the Transfer Learning technique on the VGG-19 (baseline) and customized the VGG-19 model during the training on X-Ray datasets. Pre-trained weights of the ImageNet dataset were used. We used discriminative learning rates to preserve the lower-level features and regulate the higher-level features for optimum results.

3.3.2. EfficientNetB3

We conducted our experiments on variants of the EfficientNet, i.e., EfficientNetB0, B1, B2, B3, and B4. The EfficientNet higher variants, i.e., EfficientNet B4, B5, B6, and B7, have extensive width, depth, or resolution. However, the accuracy gain was observed saturating/stable while experimenting with the X-ray datasets. In comparison to the EfficientNet-B3 model, the higher versions do not yield any relevant outcomes. Hence, detailed experiments were undertaken with the EfficientNet B1, EfficientNet B2, and EfficientNet B3 architectures. Due to significant yield accrued while experimenting on the EfficientNet-B3, we carried out binary and multi-class classification on both X-ray datasets. We trained EfficientNet CNN on 64x64 sized X-ray imaging dataset initially to obtain the weights using Progressive resizing technique [27]. These weights were transferred to the resized 128 x 128 Imaging dataset and followed by this; similar iterations were conducted repetitively by gradually increasing X-ray sizes to 256 x 256, 512 x 512. As each larger-scale model incorporated the weights from the previous iteration, it could extract more relevant features and hence demonstrated improved classification scores. This methodology yields significant results by following the strategy. Fig. 4 illustrates the implementation methodology of Transfer Learning and Progressive resizing techniques on the X-ray Images and applying the obtained weights iteratively to the forthcoming next training model with scaled-up images.

3.4. Testing

To carry out the testing, resized (H×W) size input images were given to the network to predict the output class. During testing, we used Leave-one-out (LOO) cross-validation method. In LOO-CV, the number of folds equals the number of instances in the data set. Thus, the method applied the learning iteration once for each instance while taking all

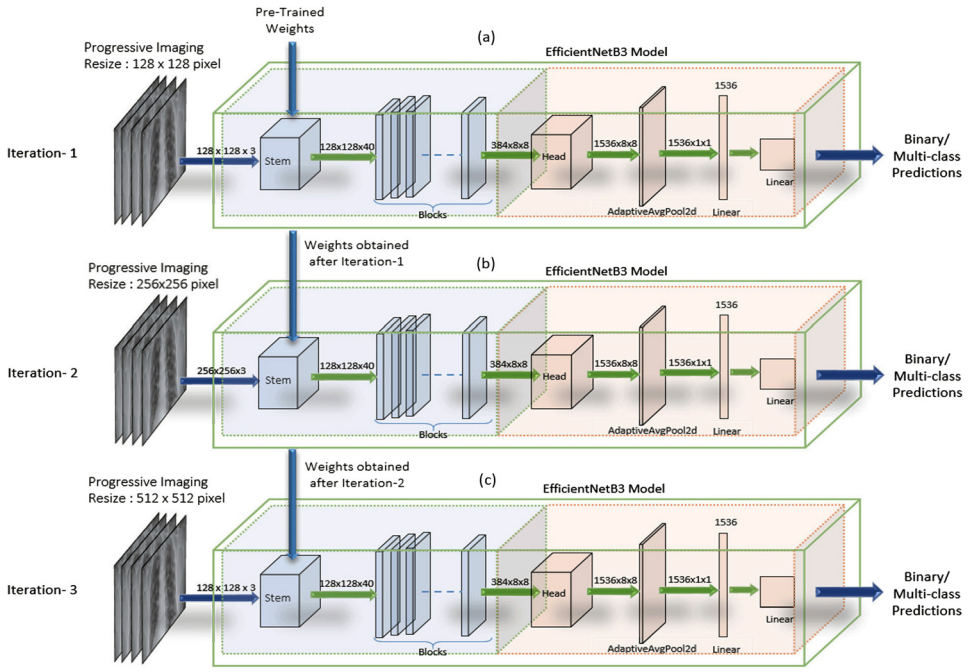

Fig. 4. The figure shows an illustrative representation of the methodology to employ the Transfer Learning technique in consultation with the Progressive Resizing Technique on the EfficientNet-B3 model. Pre-trained weights (ImageNet Dataset) transfer on the EfficientNet-B3 model with (a) (i.e., Imaging input size of 128 x 128 pixels initially), and then carry forward the obtained weights to subsequent models (b) and (c) (i.e., Imaging input size to 256 x 256 pixels and 512x512 pixels respectively).

other instances as its training set. Hence, the method ensured low bias and prevented over-fitting.

4. Discussion

4.1. Evaluation parameters

We carried out the evaluation of the model performance based on the performance metrics. The performance of the model is ascertained by the various scores, i.e., Accuracy (Acc), Precision, Sensitivity (Sens), Specificity (Spec), H-Mean, F1-score, or F-Beta. Accuracy is the overall percentage of correctly identifying COVID-19, Pneumonia, and Normal images. Sensitivity or recall measures the number of correct positive COVID-19 or specific class results to the number of all relevant samples (all positive samples). Specificity shows the ratio of the actual COVID-19 negatives to the correctly predicted as such (i.e., the patients correctly identified as not having COVID-19 consolidations). F1 Score is the Harmonic Mean between precision and recall. Kappa Score [28, 29] is a statistical measure for measuring 'Intra-rater Reliability'. We used the following measures as evaluation criteria (Abbreviations: TP- True Positive, TN- True Negative, FP- False Positive, FN- False Negative):

$$Acc = \frac{TP + TN}{TP + TN + FP + FN}$$

$$Precision = \frac{TP}{TP + FP}$$

$$Sens/Recall = \frac{TP}{TP + FN}$$

$$F1 - Score = \frac{2 * Precision * Recall}{Precision + Recall} = \frac{2 * TP}{2 * TP + FP + FN}$$

4.2. Quantitative results

We discuss the results obtained for binary and multi-class classification in this section. We used VGG-19 (Baseline) for binary classification and customized the VGG-19 model with Transfer Learning with pre-trained weights from Imagenet. Customized VGG-19 results superseded the VGG-19 (Baseline) model (with an accuracy of 89.58%) with a perfect score of 100% under all evaluation criteria. We used Transfer Learning with Progressive resizing on the EfficientNet-B3 model by progressively giving the images in 128x128, 256x256, and 512x512 sizes, and obtained an ideal score of 100% for these experiments. Table 2 illustrates the quantitative scores of the VGG-19 (baseline) viz-a-viz of VGG-19 (Customized) using transfer learning and EfficientNetB3 models' when using Transfer Learning with Progressive resizing of the X-ray images. The graphs in Fig. 5 show performance comparison under loss functions' values during the training and testing process along with Accuracy, Specificity, Sensitivity, and F1-Scores for binary classification.

Significant improvements in results were observed in feature extraction and computation efficiency when progressive resizing was used to carry out multi-class classification. We applied Transfer Learning on VGG-19 Baseline and Customised VGG-19. We experimented on EfficientNet B3 with pre-trained weights and trained them on 256x256, 512x512, and 1024 x 1024 sized progressively. The LOO cross-validation inherent zero randomnesses ensured lower bias which most negligible chances of overestimation in error rate. Hence, the results reflect no overfitting while training. Table 3 highlights the quantitative comparison of the proposed models for multi-class classification wherein the Customised VGG-19 demonstrated substantial improvement over Baseline VGG-19. The EfficientNetB3 (1024x1024) model attained the highest scores progressively and achieved perfect Precision, Recall, F1 Score, and Kappa Score (Fig. 6).

4.3. Clinical implications

Radiographs are non-invasive clinical adjuncts that play an essential role in the preliminary investigation of various pulmonary abnormalities. Especially in the COVID-19 infections, the Chest X-rays can be helpful in investigations. The exponential rise in pandemic spread makes it challenging for medical experts to carry out RT-PCR / screening tests to complete the diagnosis in time, leading to high morbidity and mortality. Since the studies reveal that the COVID-19 infected patients exhibit distinct multi-focal/bilateral ground-glass opacities and

Table 2. The table illustrates the results of the implemented models, namely VGG19 (Baseline), VGG-19 (Customized), and EfficientNetB3 with LOO and 5-Fold Cross-validation in terms of evaluations criteria (performance metrics) for Binary COVID-19 Consolidations' predictions.

Model	Acc %	Precision %	Sens %	Spec %	H-Mean %	F-Score %	AUROC %
VGG19 (Baseline)	89.58	100.0	100.0	78.26	87.80	90.91	99.30
VGG19 (Customised)	100.0	100.0	100.0	100.0	100.0	100.0	100.0
EfficientNetB3 (128x128)	100.0	100.0	100.0	100.0	100.0	100.0	100.0
EfficientNetB3 (256x256)	100.0	100.0	100.0	100.0	100.0	100.0	100.0
EfficientNetB3 (512x512)	100.0	100.0	100.0	100.0	100.0	100.0	100.0

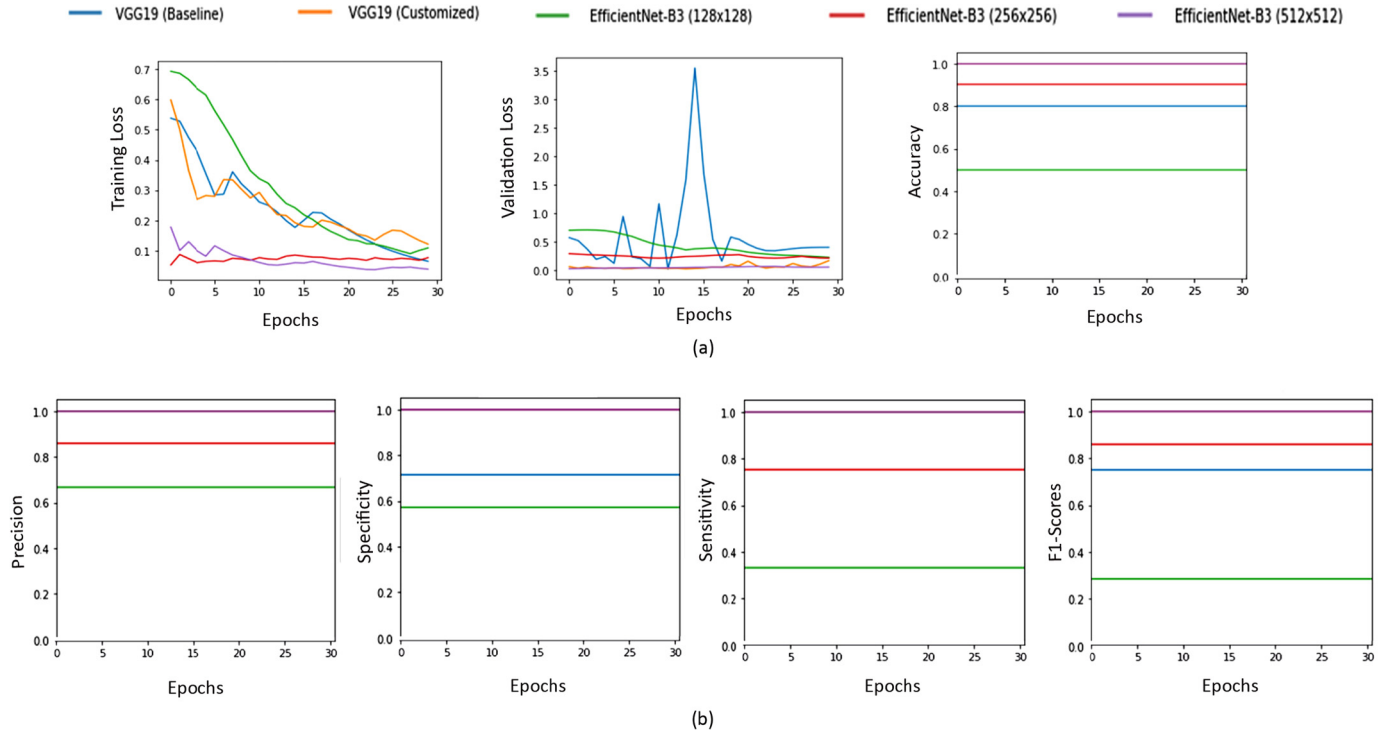

Fig. 5. The graphs illustrate the performance of the models for Binary classification for VGG-19, Customized VGG-19, and EfficientNetB3 model with (128x128), (256x256), and (512x512) resizing. From left to right, The Loss function convergence while training, and validation phase, with accuracy score shown (a). From left to right, Precision, Specificity, Sensitivity, and F1 Score indicates the enhancements achieved by the Progressive Resizing technique on EfficientNet-B3 model at (b). EfficientNet-B3 (256x256) and Customised VGG19 yield nearly perfect scores on all evaluation criteria, while baseline VGG-19 suffered overfitting.

Table 3. The table illustrates the results of the implemented models attained on VGG-19 (Customized) by applying Transfer Learning and EfficientNetB3 by applying the Progressive Resizing Technique with 128x128, 256x256, and 512x512 pixel sized Imaging, in terms of performance scores for Multi-class Consolidations' predictions.

Model	Imaging dimension	Acc %	Precision %	Recall %	F-Score %	Kappa score %
VGG19 (Baseline)	-	64.58	65.33	52.54	44.38	69.64
VGG19 (Customised)	-	97.37	97.37	97.33	97.33	97.28
EfficientNetB3	256 x 256	98.36	97.22	98.41	98.17	98.96
EfficientNetB3	512 x 512	96.72	97.10	97.10	97.10	97.40
EfficientNetB3	1024x1024	100.0	100.0	100.0	100.0	100.0

patchy reticular (or reticulonodular) opacities with ground glass patterns, a well trained ConvNet model can act as an alternative screening modality for identifying COVID-19 and validation during diagnosis. The proposed methodology has demonstrated enhancements in identifying COVID-19 consolidations, prioritizing patient care, and allotment of resources.

4.4. Saliency maps

We used Grad-CAM, which uses the gradients of any target class concept, e.g., COVID-19 consolidations, flowing into the final convolutional layer. Finally, it produces a coarse localization map highlighting the important regions in the X-ray image for predicting the class. Gradient-

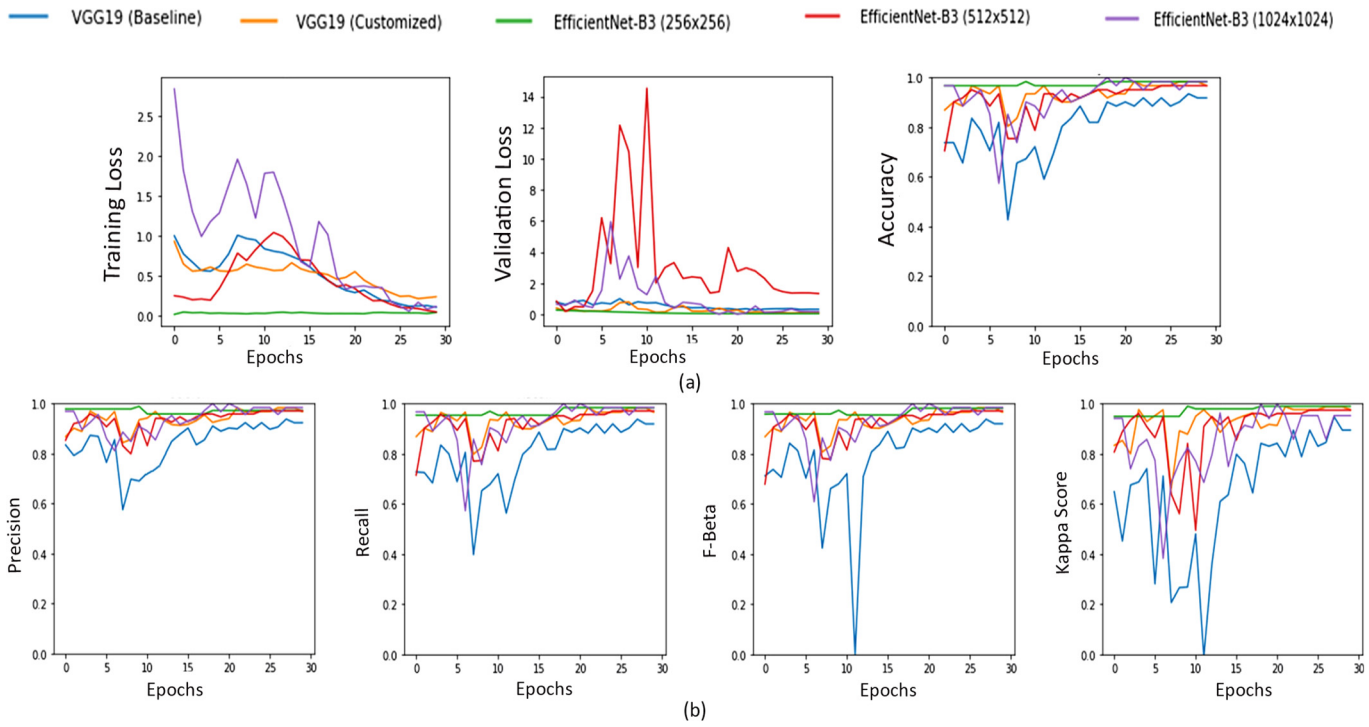

Fig. 6. The graphs illustrate the performance of the models for Multi-class classification for VGG-19, Customized VGG-19, and EfficientNetB3 model with (128x128), (256x256), and (512x512) resizing. From left to right, The Loss function convergence while training, and validation phase, with the accuracy score shown at (a). From left to right, Precision, Recall, F-beta, and Kappa Score indicates the enhancements achieved by the Progressive Resizing technique on EfficientNet-B3 model at (b). The results demonstrated that Customised VGG19 supersedes Baseline VGG-19 and EfficientNet-B3 (256x256) and EfficientNet-B3 (1024x1024) yield nearly perfect scores on all evaluation criteria.

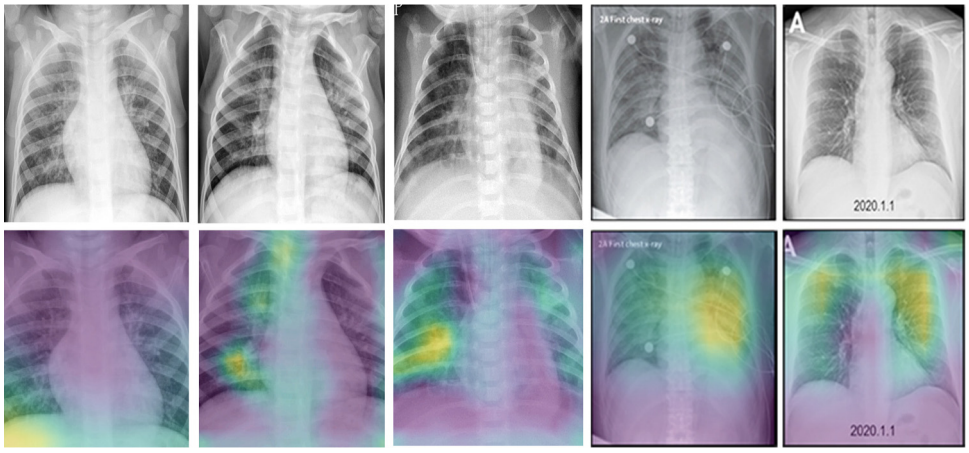

Fig. 7. The figure illustrates the input Chest X-Ray Imaging with Model generated Gradient-weighted Class Activation Maps below the inputs, respectively. Input X-Ray Imaging and Saliency Map at (a) Predicts in class 'Normal,' (b), and (c) show the predictions of Pneumonia, while (d) and (e) show the predictions of COVID-19 consolidations.

weighted Class Activation Map (Grad-CAM) enhances the assimilation of the results by highlighting the relevant regions from which the results have been predicted [30]. We took the average of all the 1x1x512 channels in Adaptive Average Pooling to generate the Saliency maps, followed by conversion to a tensor of 512. The generated tensor was then multiplied with a matrix of size (512 x no. of classes) to obtain the final visualization output. In our multi-class experiments, the 512 values represented the features extracted in the form of matrices for three different classes. We took the first class's average across every channel to show activated area when the final layer has produced a prediction for any specific class. The activated area is shown with yellow, cyan, and magenta color in decreasing order of values, which contributed to the X-ray image classification. Fig. 7 shows the Grad-CAM activation area for various class inputs by highlighting the relevant features learned from opacities in X-rays.

5. Conclusion

We proposed a novel methodology to enhance the classification pipeline to identify pneumonia and COVID-19 infections by analyzing pulmonary consolidations in Chest X-rays. Our experiments highlight the novel employment of Progressive Resizing techniques on CNNs to carry out effective medical imaging-based diagnostics. The developed models can act as a second opinion aid in prioritizing the patients' care. The proposed novel approach on Deep Neural Network models enhances the performance significantly. The proposed pipeline starts

with the Chest Consolidation recognition stage, where we used VGG-19 (Baseline) and EfficientNet-B3 (Baseline) models to carry out binary and multi-class classifications on both datasets. We modified and fine-tuned the Baseline VGG-19 architecture, demonstrating a significant increase in performance scores in binary classification. In binary and multi-class classification experiments, the Customized VGG-19 and EfficientNet-B3 attained unity scores. Later, we used Transfer Learning and Progressive Resizing techniques on EfficientNet-B3 for multi-class classification, which showed promising results by achieving benchmark scores on X-ray images, i.e., 100% accuracy, 100% precision, 100% recall, 100% specificities, and 100% F-Beta score. The GradCam based visualization, with the help of saliency maps, extends transparency in correlating model predictions. Clinical implications exist in peripheral health centers with a lack of trained human resources to interpret radiological investigations' for classifying SARS, MERS, pneumonia, and COVID-19.

Declarations

Author contribution statement

Anant Bhatt: Conceived and designed the experiments; Performed the experiments; Analyzed and interpreted the data; Wrote the paper.

Ketan Kotecha: Conceived and designed the experiments; Contributed reagents, materials, analysis tools or data.

Amit Ganatra: Analyzed and interpreted the data; Contributed reagents, materials, analysis tools or data.

Funding statement

This research did not receive any specific grant from funding agencies in the public, commercial, or not-for-profit sectors.

Data availability statement

Data included in article/supplementary material/referenced in article.

Declaration of interests statement

The authors declare no conflict of interest.

Additional information

No additional information is available for this paper.

References

[1] WHO, World health organisation coronavirus disease (COVID-19) pandemic, https://www.who.int/emergencies/diseases/novel-coronavirus-2019, 2020. (Accessed 9 April 2020).

[2] F. Song, N. Shi, F. Shan, Z. Zhang, J. Shen, H. Lu, Y. Ling, Y. Jiang, Y. Shi, Emerging 2019 novel coronavirus (2019-nCoV) pneumonia, Radiology 295 (1) (2020) 210–217.

[3] G.E. Antonio, K.T. Wong, E.L. Tsui, D.P. Chan, D.S. Hui, A.W. Ng, K.K. Shing, E.H. Yuen, J.C. Chan, A.T. Ahuja, Chest radiograph scores as potential prognostic indicators in severe acute respiratory syndrome (SARS), Am. J. Roentgenol. 184 (3) (2005) 734–741.

[4] L. Ketai, N.S. Paul, T.W. Ka-tak, Radiology of severe acute respiratory syndrome (SARS): the emerging pathologic-radiologic correlates of an emerging disease, J. Thorac. Imaging 21 (4) (2006) 276–283.

[5] K.M. Das, E.Y. Lee, R. Singh, M.A. Enani, K. Al Dossari, K. Van Gorkom, S.G. Larsson, R.D. Langer, Follow-up chest radiographic findings in patients with MERS-CoV after recovery, Indian J. Radiol. Imaging 27 (3) (2017) 342.

[6] M. Cascella, M. Rajnik, A. Aleem, S. Dulebohn, R. Di Napoli, Features, Evaluation, and Treatment of Coronavirus (COVID-19), StatPearls, 2021.

[7] M.M. de Gracia, Imaging the coronavirus disease COVID-19, https://healthcare-in-europe.com/en/news/imaging-the-coronavirus-disease-covid-19.html, 2020.

[8] M. Hosseiny, S. Kooraki, A. Gholamrezanezhad, S. Reddy, L. Myers, Radiology perspective of coronavirus disease 2019 (COVID-19): lessons from severe acute respiratory syndrome and Middle East respiratory syndrome, Am. J. Roentgenol. 214 (5) (2020) 1078–1082.

[9] D.J. Cohen, COVID chestxray dataset, https://github.com/ieee8023/covid-chestxray-dataset, Mar. 2020.

[10] T. Ozturk, M. Talo, E.A. Yildirim, U.B. Baloglu, O. Yildirim, U.R. Acharya, Automated detection of COVID-19 cases using deep neural networks with X-ray images, Comput. Biol. Med. 121 (2020) 103792.

[11] H. Panwar, P. Gupta, M.K. Siddiqui, R. Morales-Menendez, V. Singh, Application of deep learning for fast detection of COVID-19 in X-rays using nCOVnet, Chaos Solitons Fractals 138 (2020) 109944.

[12] E.E.-D. Hemdan, M.A. Shouman, M.E. Karar, COVIDX-Net: a framework of deep learning classifiers to diagnose COVID-19 in X-ray images, arXiv preprint, arXiv: 2003.11055, 2020.

[13] A. Abbas, M.M. Abdelsamea, M.M. Gaber, Classification of COVID-19 in chest X-ray images using DeTraC deep convolutional neural network, Appl. Intell. 51 (2) (2021) 854–864.

[14] K. Santosh, AI-driven tools for coronavirus outbreak: need of active learning and cross-population train/test models on multitudinal/multimodal data, J. Med. Syst. 44 (5) (2020) 1–5.

[15] D. Das, K. Santosh, U. Pal, Truncated inception net: COVID-19 outbreak screening using chest X-rays, Phys. Eng. Sci. Med. 43 (3) (2020) 915–925.

[16] H. Mukherjee, S. Ghosh, A. Dhar, S.M. Obaidullah, K. Santosh, K. Roy, Shallow convolutional neural network for COVID-19 outbreak screening using chest X-rays, Cogn. Comput. (2021) 1–14.

[17] M. Toğaçar, B. Ergen, Z. Cömert, COVID-19 detection using deep learning models to exploit social mimic optimization and structured chest X-ray images using fuzzy color and stacking approaches, Comput. Biol. Med. 121 (2020) 103805.

[18] A.R. Bhatt, A. Ganatra, K. Kotecha, Cervical cancer detection in pap smear whole slide images using ConvNet with transfer learning and progressive resizing, PeerJ Comput. Sci. 7 (2021) e348.

[19] V. COVID-Net team, C. Image Processing Research Group, University of Waterloo, C. DarwinAI Corp., COVID-Net open source initiative, https://github.com/lindawangg/COVID-Net, Apr. 2020.

[20] K. Simonyan, A. Zisserman, Very deep convolutional networks for large-scale image recognition, arXiv preprint, arXiv:1409.1556, 2014.

[21] M. Tan, Q. Le, EfficientNet: rethinking model scaling for convolutional neural networks, in: International Conference on Machine Learning, PMLR, 2019, pp. 6105–6114.

[22] G. Huang, Z. Liu, L. Van Der Maaten, K.Q. Weinberger, Densely connected convolutional networks, in: Proceedings of the IEEE Conference on Computer Vision and Pattern Recognition, 2017, pp. 4700–4708.

[23] S.J. Pan, Q. Yang, A survey on transfer learning, IEEE Trans. Knowl. Data Eng. 22 (10) (2009) 1345–1359.

[24] J. Yosinski, J. Clune, Y. Bengio, H. Lipson, How transferable are features in deep neural networks?, arXiv preprint, arXiv:1411.1792, 2014.

[25] I. Loshchilov, F. Hutter, Fixing weight decay regularization in Adam, https://openreview.net/forum?id=rk6qdGgCZ, 2018.

[26] L.N. Smith, N. Topin, Super-convergence: very fast training of neural networks using large learning rates, in: Artificial Intelligence and Machine Learning for Multi-Domain Operations Applications, vol. 11006, International Society for Optics and Photonics, 2019, p. 1100612.

[27] J. Howard, S. Gugger, Fastai: a layered API for deep learning, Information 11 (2) (2020) 108.

[28] J. Cohen, A coefficient of agreement for nominal scales, Educ. Psychol. Meas. 20 (1) (1960) 37–46.

[29] J. Cohen, Weighted kappa: nominal scale agreement with provision for scaled disagreement or partial credit, Psychol. Bull. 70 (1968) 213–220.

[30] R.R. Selvaraju, M. Cogswell, A. Das, R. Vedantam, D. Parikh, D. Batra, Grad-CAM: visual explanations from deep networks via gradient-based localization, in: Proceedings of the IEEE International Conference on Computer Vision, 2017, pp. 618–626.